Elastic-driven instabilities in microfluidic flow-focusing devices

M. S. N. Oliveira[1], F. T. Pinho[2], M. A. Alves[1]

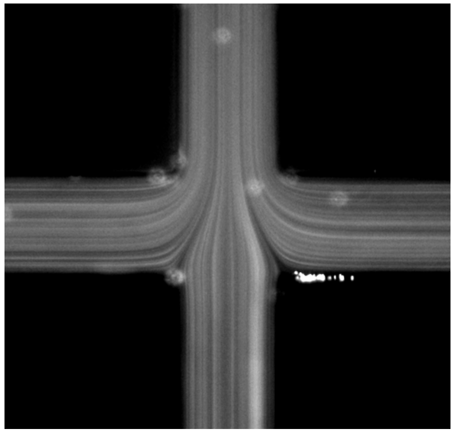

1: Departamento de Engenharia Química, CEFT
Faculdade de Engenharia da Universidade do Porto
Rua Dr. Roberto Frias, 4200-465 Porto, Portugal
e-mail: {mmalves, monica.oliveira}@fe.up.pt
web: http://www.fe.up.pt/~ceft

2: Departamento de Engenharia Mecânica, CEFT
Faculdade de Engenharia da Universidade do Porto
Rua Dr. Roberto Frias, 4200-465 Porto, Portugal
e-mail: fpinho@fe.up.pt
web: http://www.fe.up.pt/~ceft

Universidade do Porto
Faculdade de Engenharia
FEUP

Instabilities at the microscale: **Cross-Slot**

- Experimental

PRL **96,** 144502 (2006) PHYSICAL REVIEW LETTERS

Elastic Instabilities of Polymer Solutions in Cross-Channel Flow

P. E. Arratia,[1,2] C. C. Thomas,[1] J. Diorio,[1] and J. P. Gollub[1,2]

Newtonian: Re < 10^{-2}

PAA Boger fluid: Re < 10^{-2} (De=4.5)

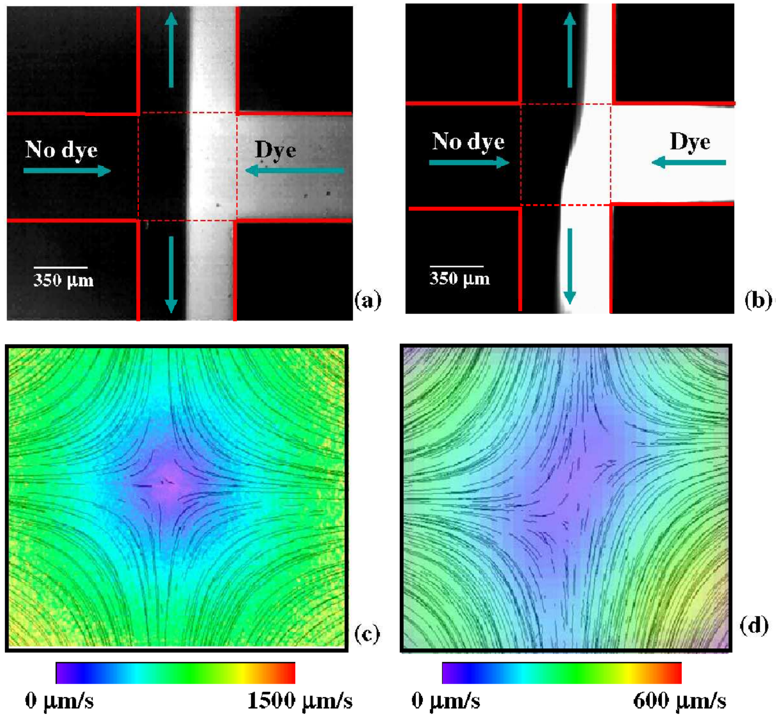

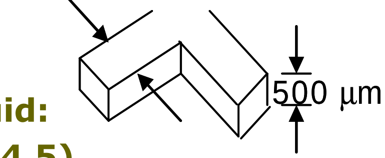

- Numerical

PRL **99,** 164503 (2007) PHYSICAL REVIEW LETTERS

Purely Elastic Flow Asymmetries

R. J. Poole,[1] M. A. Alves,[2] and P. J. Oliveira[3]

UCM model

2D, Creeping Flow

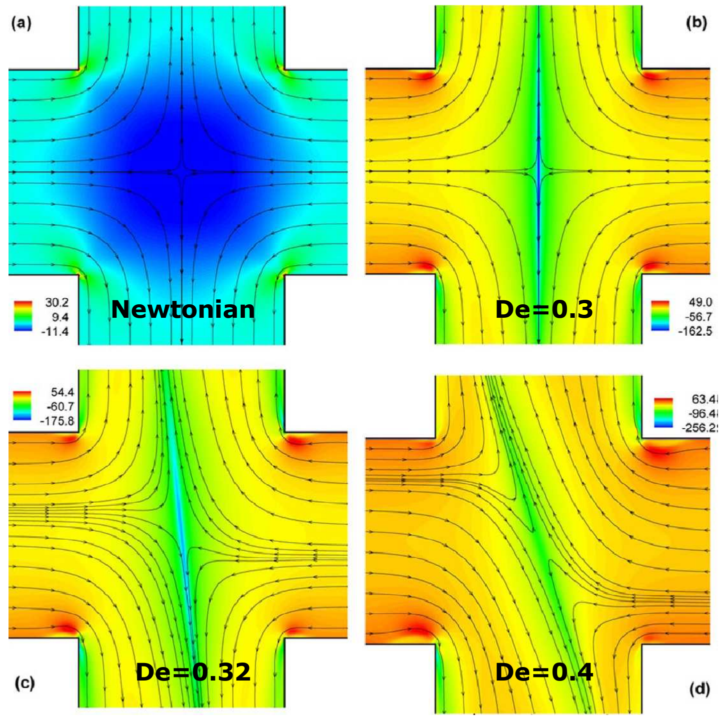

Instabilities at the microscale: **T-Channel**

J. Non-Newtonian Fluid Mech. 163 (2009) 9–24

Investigating the stability of viscoelastic stagnation flows in T-shaped microchannels

J. Soulages[a,*], M.S.N. Oliveira[b], P.C. Sousa[b], M.A. Alves[b], G.H. McKinley[a,*]

0.075 wt. % PEO in glycerol/water solution (60/40 wt. %)

Without Cavity

Pinned stagnation point

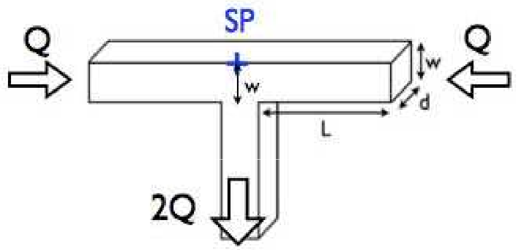

With Cavity

Free stagnation point

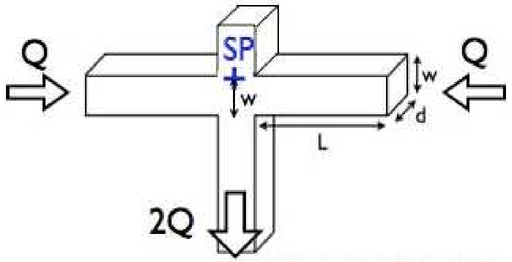

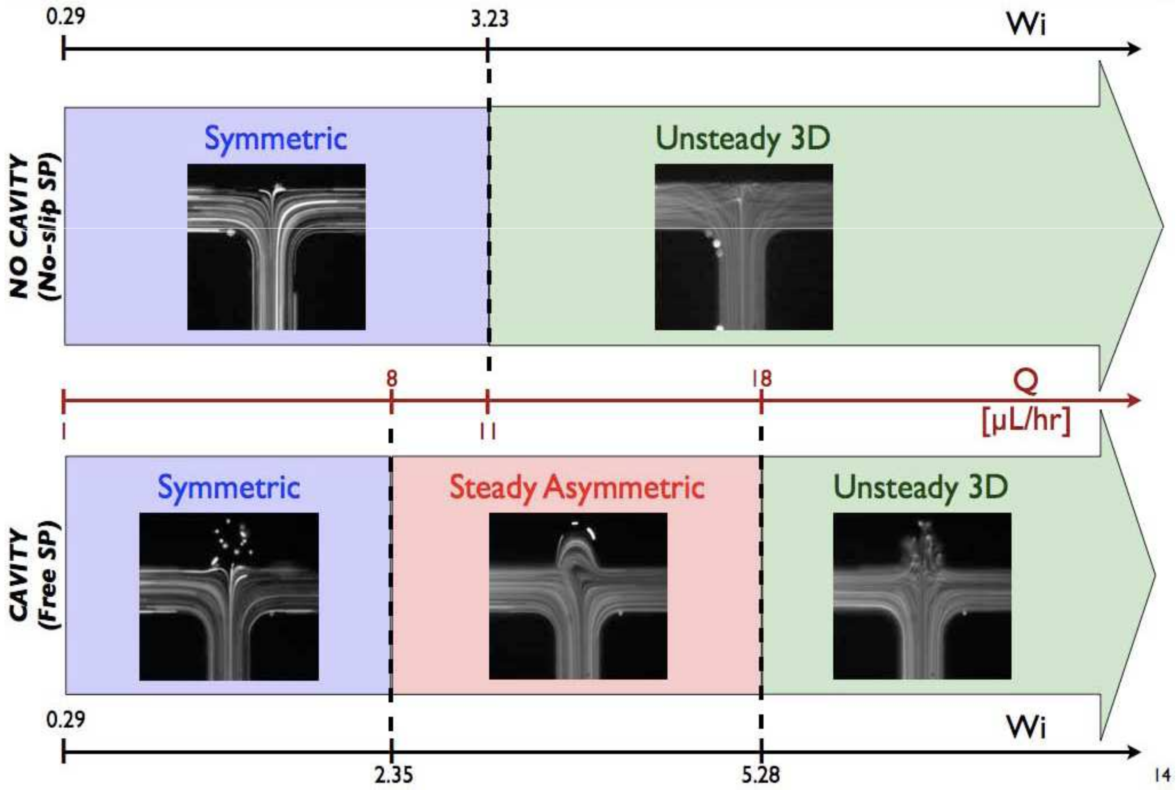

Flow focusing geometry

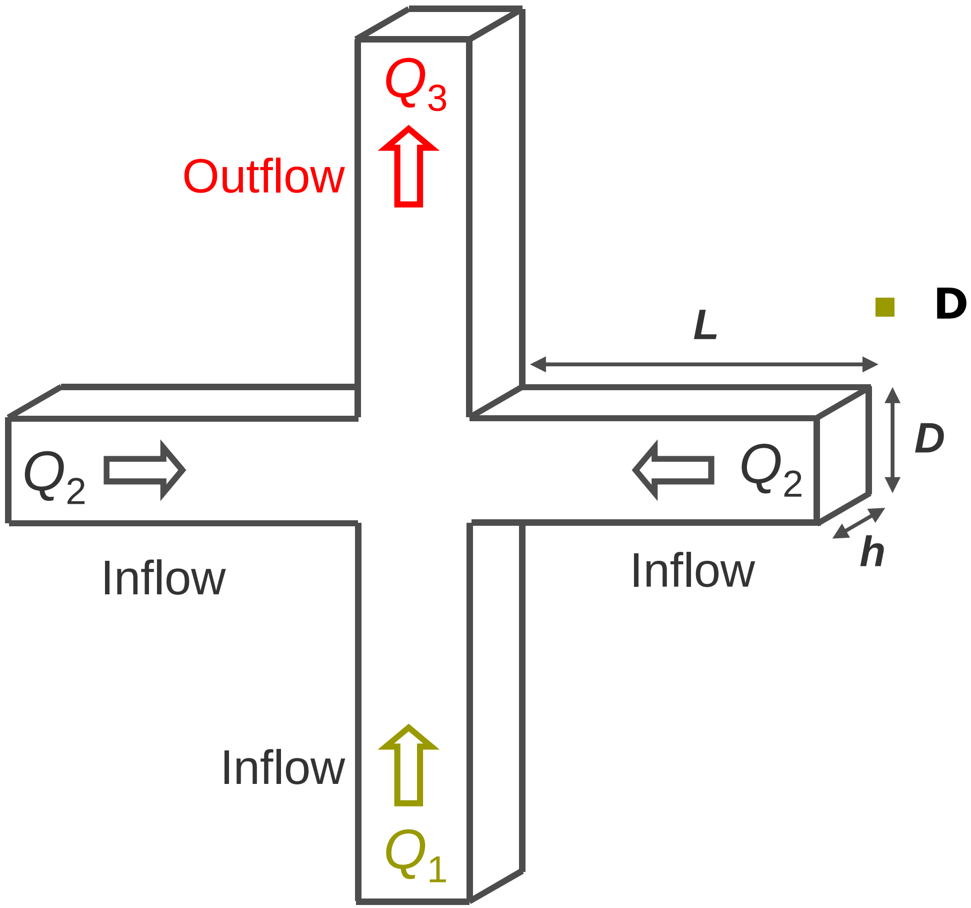

Cross-slot geometry
with **3 inlets** and **1 outlet**

- **Operational Variables**

Q_1, Q_2

⬇

$Q_3 = 2 \times Q_2 + Q_1$

- **Dimensionless Variables**

$FR = Q_2 / Q_1$

$VR = U_2 / U_1 \; (= FR)$

$$Re = \frac{\rho U_2 D}{\eta_0}, \quad De = \lambda \frac{U_2}{D} \quad \Bigg\} \quad El = \frac{De}{Re}$$

- **Channel dimensions:**
  - kept constant for all experiments and numerical calculations
  - Equal dimensions for all inlet/outlet arms

Fabrication process: **soft lithography**

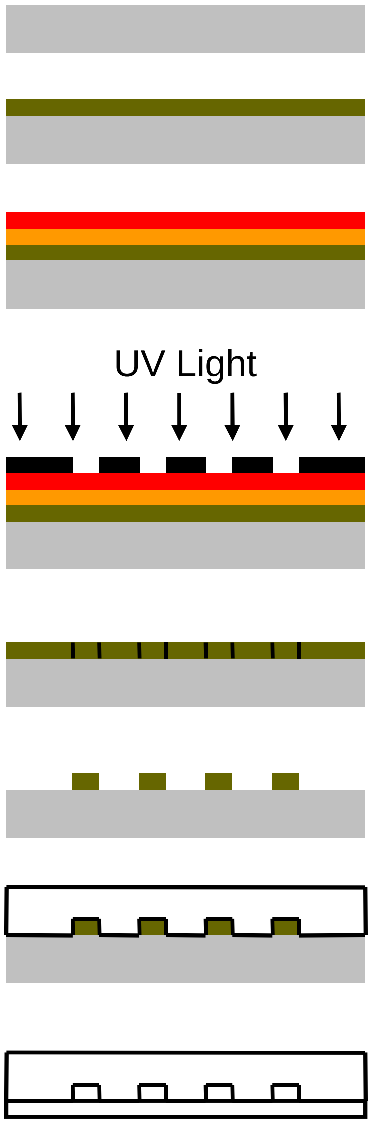

1. **Silicon Wafer**
2. Spin coat photoresist **SU-8** and prebake
3. Spin coat **barrier coat (CEM-BC7.5)** and **contrast enhancer (CEM 388SS)** (vertical walls).
4. **Chrome Mask** over coated wafer
5. **UV Exposure** – **cross-link SU-8**
6. Wash **barrier coat** and **contrast enhancer**
7. Post-bake and develop **SU-8**
8. Pour **PDMS** over substrate and cure (80^{o}C, 25 mins)
9. Peel off substrate
10. Seal with glass slide covered with PDMS

- **Microchannels**:
  - Planar geometry
  - Square cross-section
  - Nearly vertical walls
  - Accuracy of channels to within 5%

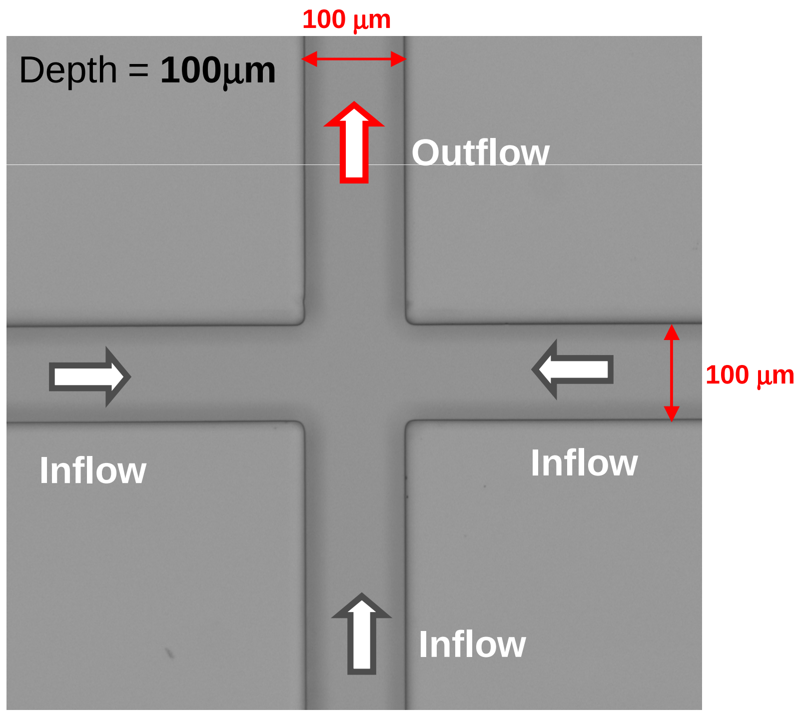

Y. Xia and G. M. Whitesides, Annu Rev. Mater. Sci. 1998, 28:153-84

Experimental set-up

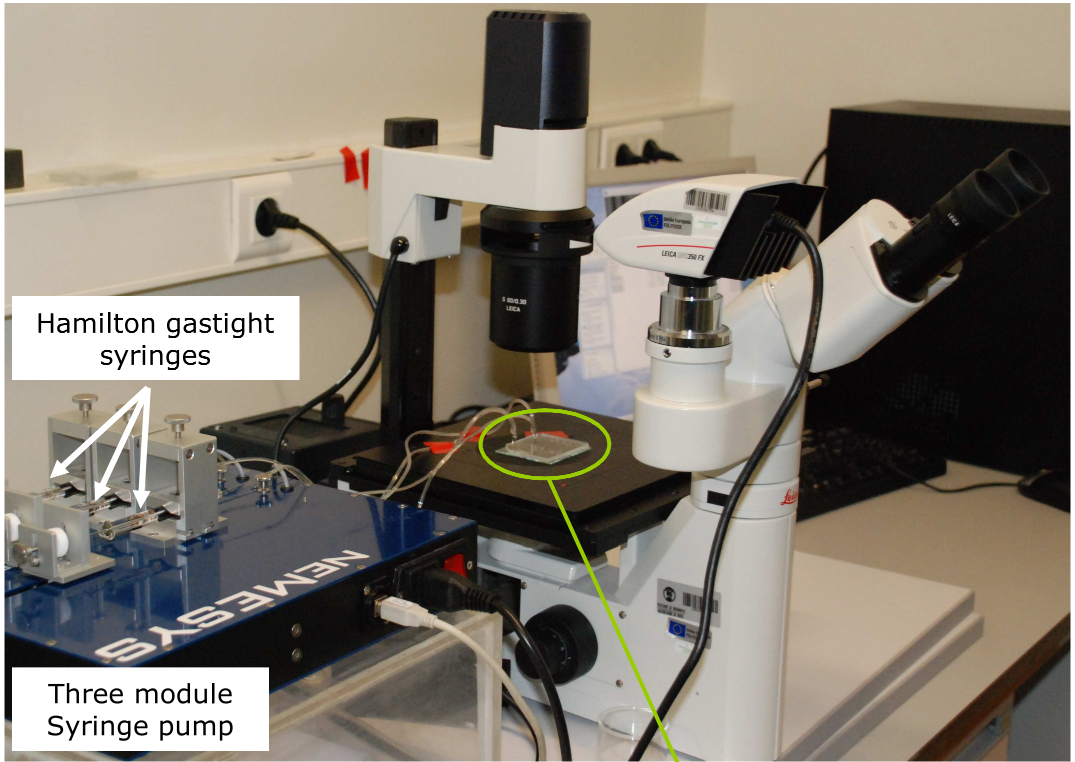

Visualizations

Microscope:
Leica, DMI LED

Camera:
Leica, DFC 350X

Objective lens:
10× objective
NA=0.3 (δz=30μm)

Illumination:
Mercury lamp (λ=532nm)

Filter Cube:
Emission filter: BP 530-545 nm
Dichroic mirror: 565 nm
Barrier filter: 610-675 nm

Tracers:
1.1μm Nile red fluorescent particles (Ex/Em: 520/580 nm)

Additives:
SDS (0.1 wt.%)

Flow

Syringe pump:
CETONI, neMESYS
with 3 independent modules

Flow rate:
$0.001 \leq Q \leq 3$ ml/h

Syringes:
Hamilton Gastight syringes

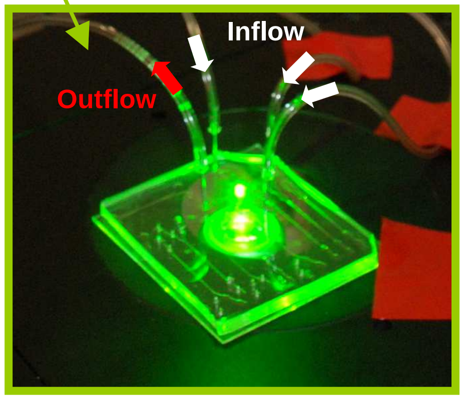

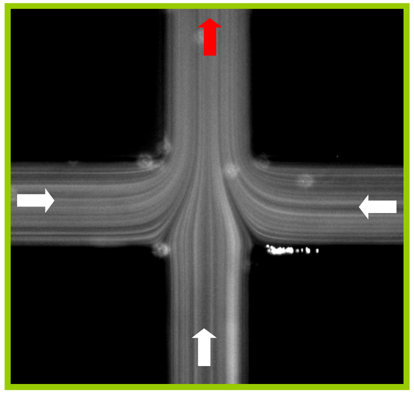

Shear Rheology

- Viscoelastic Fluid:

  Aqueous solution of **PAA** (M_w=18x10^6 g/mol)

  - **PAA 125 + NaCl**
    125 ppm PAA
    + 1% NaCl (*wt*)
    + 0.1% SDS (*wt*)

- Newtonian Fluid:

  - **Water**
    Water
    + 0.1% SDS (*wt*)

Steady Shear

Anton Paar, model Physica MCR 301

Cone-and-plate geometry (d=75mm, 1º)

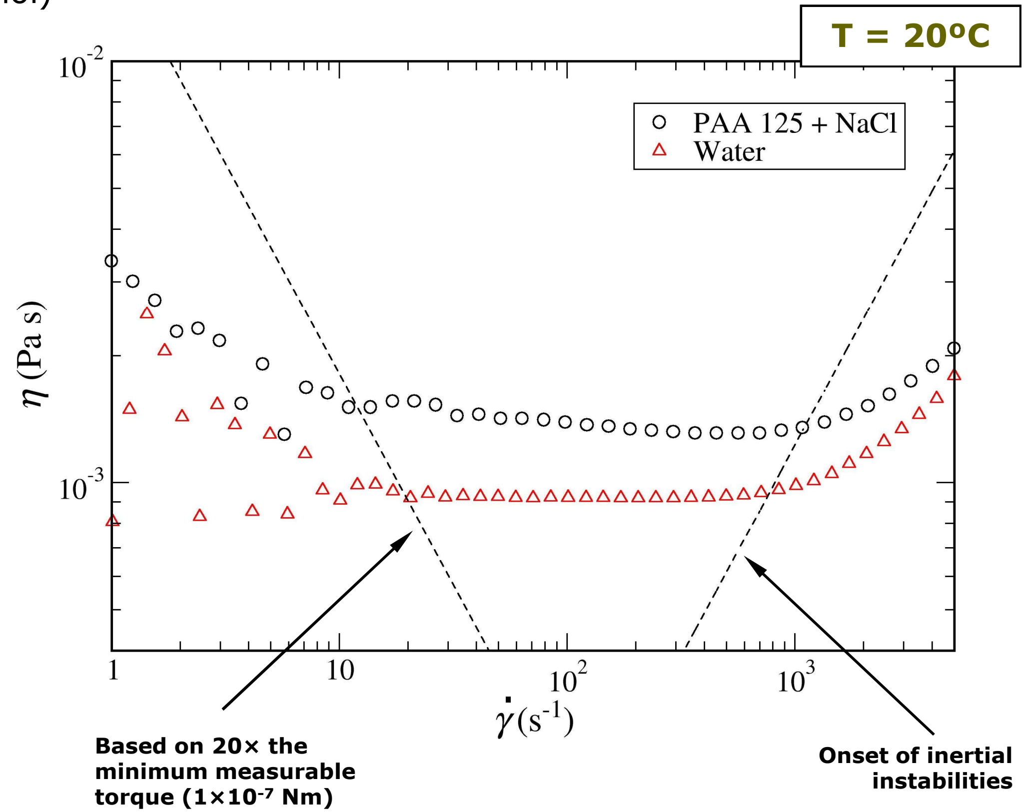

Extensional Rheology

Extensional Rheology
Haake CaBER 1, Thermo Electron Corporation
(D_p = 6 mm)

Aspect ratios: $\Lambda_i = D_i/D_p = 0.33$
$\Lambda_f = D_f/D_p = 1.56$

Imposed strain: $\varepsilon = \ln(\Lambda_f/\Lambda_i) = 1.53$

Fluid properties

PAA 125 + NaCl		
Zero-shear rate viscosity	η_0 [Pa s]	0.00131
CaBER relaxation time	λ_{CaBER} [ms]	12.4±0.2
Density	ρ [kg/m^3]	1005

T = 20ºC

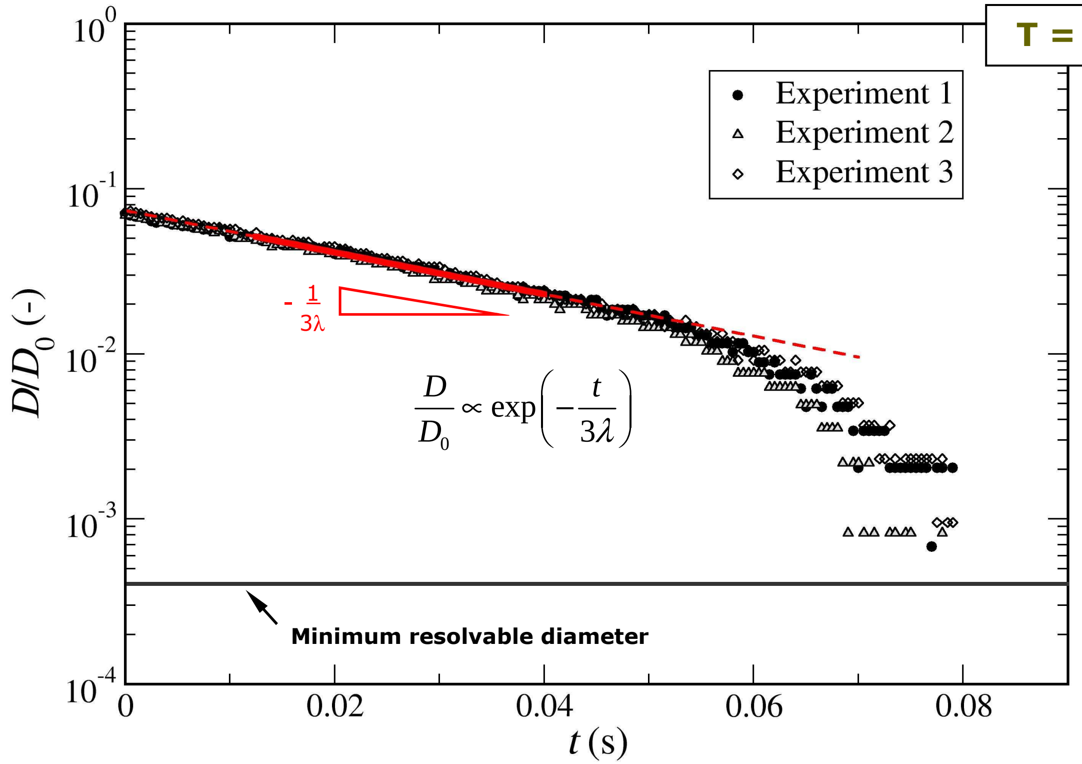

Governing equations

- Isothermal Incompressible Flow

$$\nabla \cdot \mathbf{u} = 0$$

Conservation of mass

$$-\nabla p + \nabla \cdot \boldsymbol{\tau} + \eta_s \nabla^2 \mathbf{u} = \mathbf{0}$$

Conservation of momentum

- Constitutive Equations

$$\left[1 + \frac{\lambda \varepsilon}{\eta_p} \mathrm{tr}(\boldsymbol{\tau})\right] \boldsymbol{\tau} + \lambda \overset{\nabla}{\boldsymbol{\tau}} = 2\eta_p \mathbf{D}$$

Simplified PTT model

ε= 0

$$\boldsymbol{\tau} + \lambda \overset{\nabla}{\boldsymbol{\tau}} = 2\eta_p \mathbf{D}$$

Oldroyd-B model

η_s= 0

$$\boldsymbol{\tau} + \lambda \overset{\nabla}{\boldsymbol{\tau}} = 2\eta \mathbf{D}$$

UCM model

λ = 0

$$\boldsymbol{\tau} = 2\mu \mathbf{D}$$

Newtonian fluid

Numerical method

- **Finite Volume Method**, using a time-marching algorithm*
  - Governing equations discretized in time over a small time step, δt
  - Differential equations integrated over control volumes, CV

*Oliveira et al., JNNFM,79 (1998) 1-43

- **Log-conformation approach**** to solve the equivalent form of the constitutive equation containing an evolution equation of the conformation tensor.

**Fattal and Kupferman, JNNFM, 123 (2004) 281-285
Afonso et al., JNNFM, *submitted* (2008)

- Implicit first-order Euler scheme for time-derivative discretization.

- Central differences for discretization of diffusive terms.

- **CUBISTA***** high-resolution scheme for discretization of the advective terms of the momentum equations.

***Alves et al., Int. J. Num. Methods in Fluids, 122 (2003) 47-75

- Pressure-velocity and velocity-stress coupling ensured at the CV faces – SIMPLEC algorithm****

****Patankar and Spalding, Int. J. Heat and Mass Transfer, 15 (1972) 1787–806

- The ensemble of all control volumes defines the computational mesh.

Numerical mesh and boundary conditions

- **Mesh Characteristics**:
  - Two-dimensional
  - Structured, orthogonal and non-uniform
  - Dimensions equal to the experiments

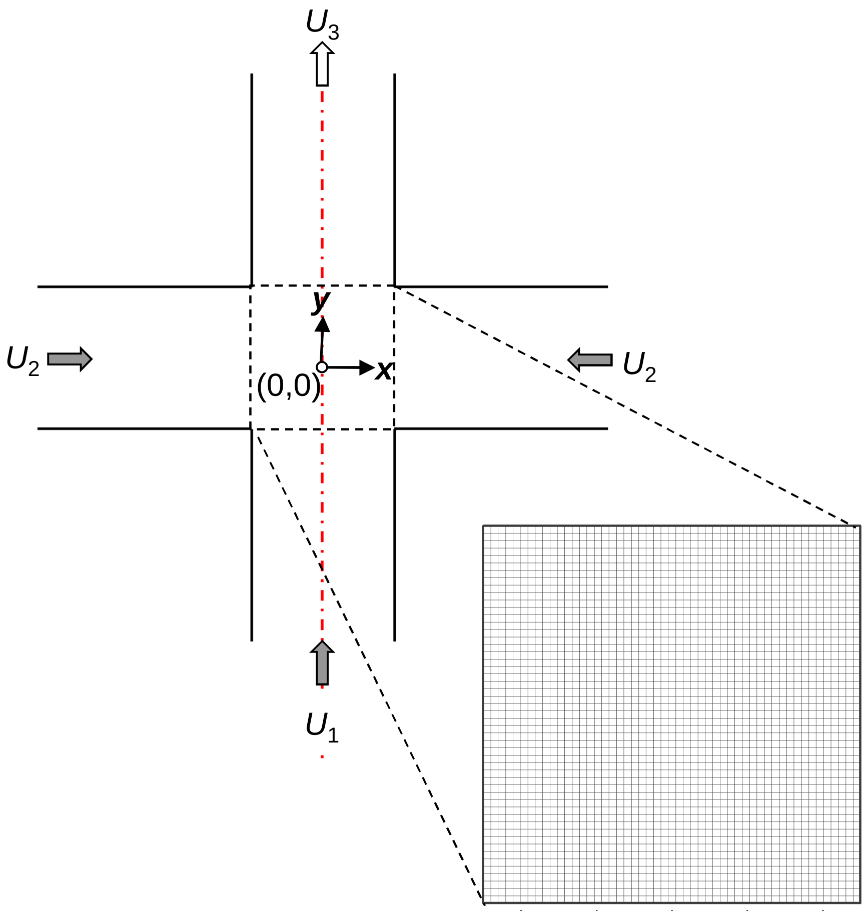

- **Boundary Conditions**:
  - INLET
    - Fully-developed velocity profile
    - Null stress components
  - OUTLET
    - Vanishing streamwise gradients of velocity and stress components
    - Constant pressure gradient
  - WALLS
    - No-slip conditions

Standard Mesh used

(more refined meshes also used)

Geometry	NCells	Δx_{min}, Δy_{min} Δz_{min}
2D	23001	0.02D

Converging Flow

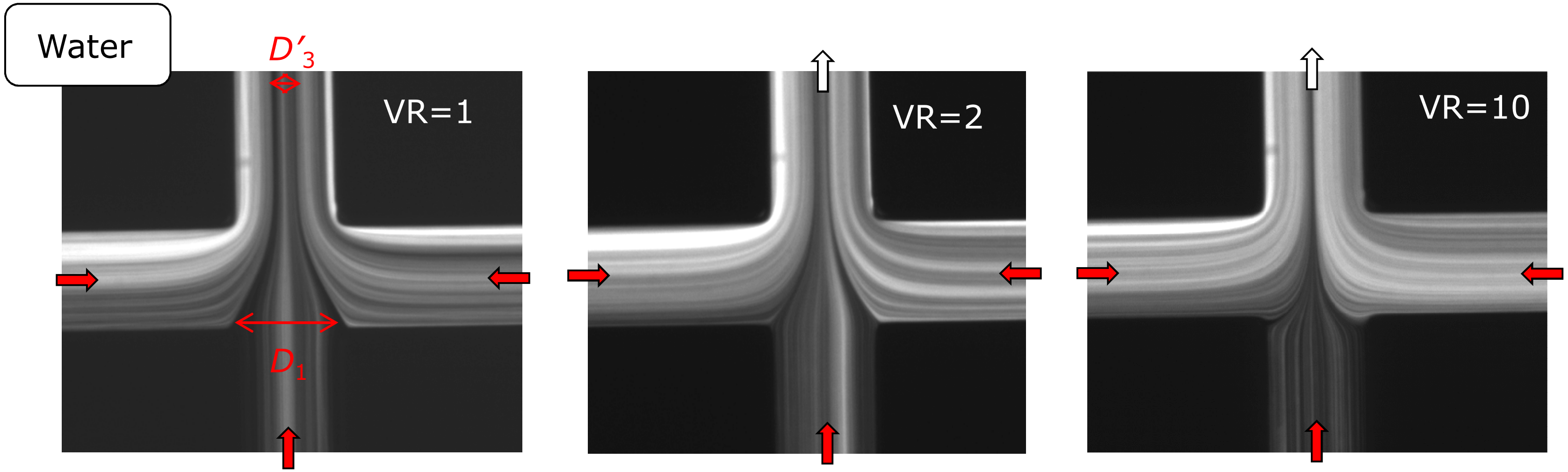

- Two opposing lateral streams shape a third inlet stream
- Converging flow region
- Separation streamlines naturally evolve to a nearly hyperbolic shape
- Hencky strain controlled by operating parameters:

$$\varepsilon_H = \ln\left(\frac{D_1}{D_3^{'}}\right) = \ln\left[\frac{3}{2}\left(1 + 2 \cdot VR\right)\right]$$

- Approximately constant strain rate at the centerline

Converging Flow

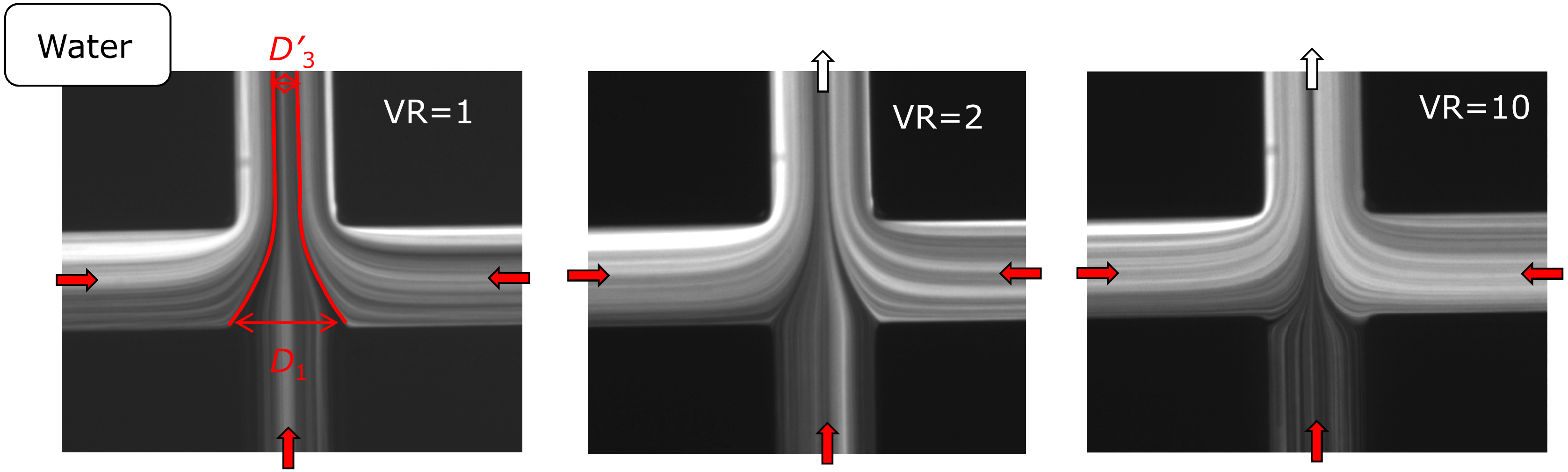

- Two opposing lateral streams shape a third inlet stream
- Converging flow region
- Separation streamlines naturally evolve to a nearly hyperbolic shape
- Hencky strain controlled by operating parameters:

$$\varepsilon_H = \ln\left(\frac{D_1}{D_3^{'}}\right) = \ln\left[\frac{3}{2}\left(1 + 2 \cdot VR\right)\right]$$

- Approximately constant strain rate at the centerline

Instabilities at the microscale

J. Non-Newtonian Fluid Mech. 160 (2009) 31–39

Purely elastic flow asymmetries in flow-focusing devices

M.S.N. Oliveira[a,*], F.T. Pinho[b], R.J. Poole[c], P.J. Oliveira[d], M.A. Alves[a]

UCM model
2D, Creeping Flow

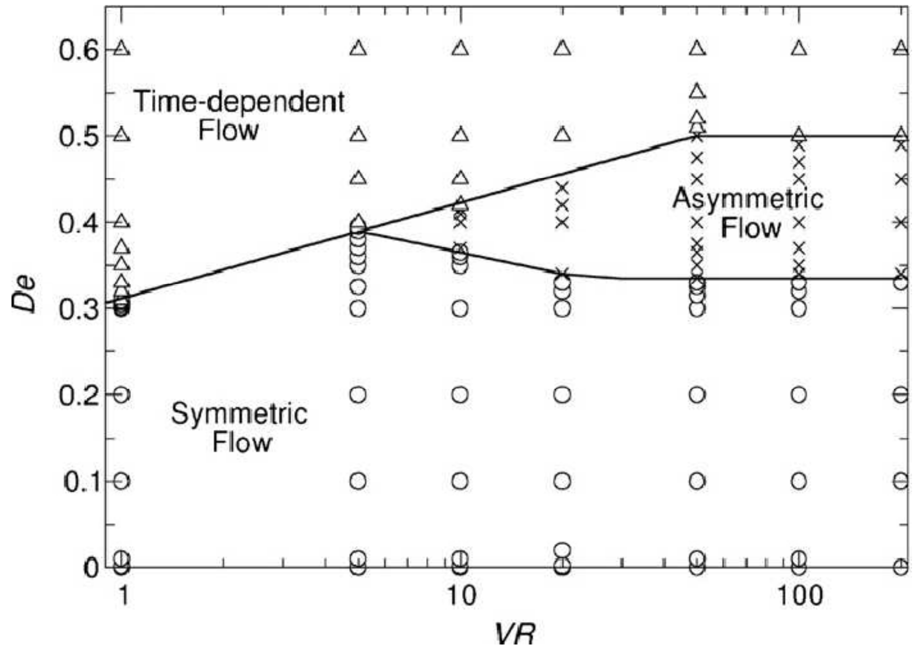

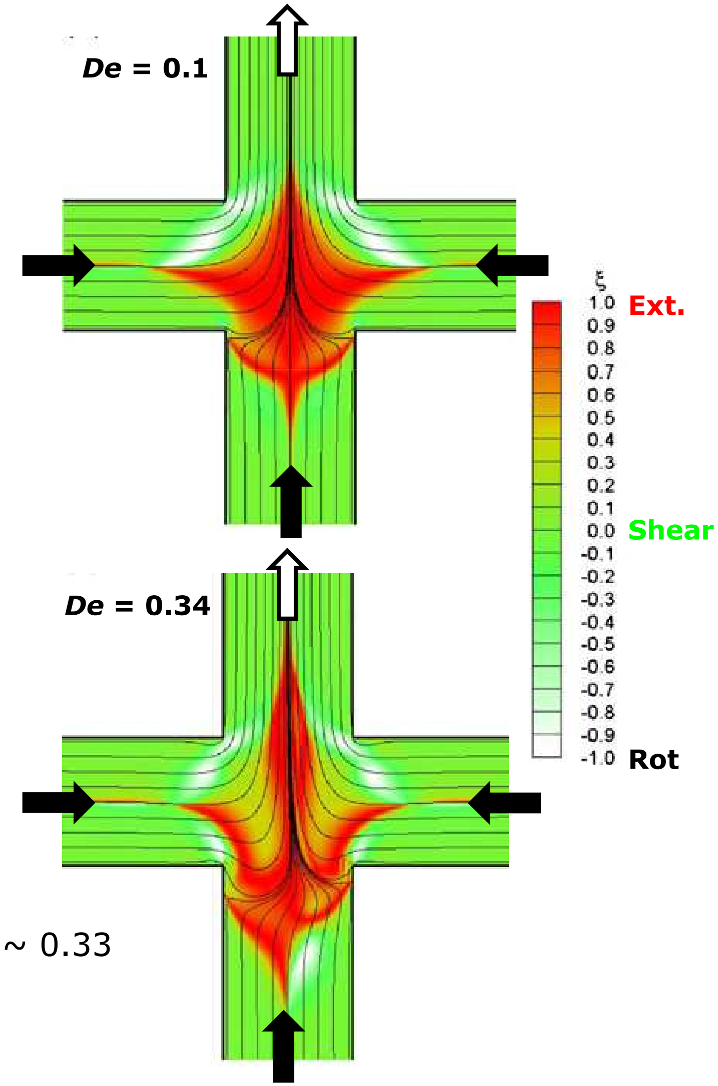

- For **low** VR: asymmetric flow not observed
- For **high** VR: **symmetric** → **asymmetric** → **oscillatory**
  - The **critical De_c** becomes approximately **constant**: $De_c \sim 0.33$
  - **Bistable** flow

Effect of *VR* on the degree of asymmetry

Effect of VR
UCM Model
2D, Creeping Flow

$$F^* = \frac{F_W - F_E}{F_3}$$

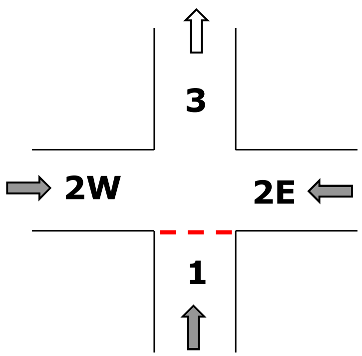

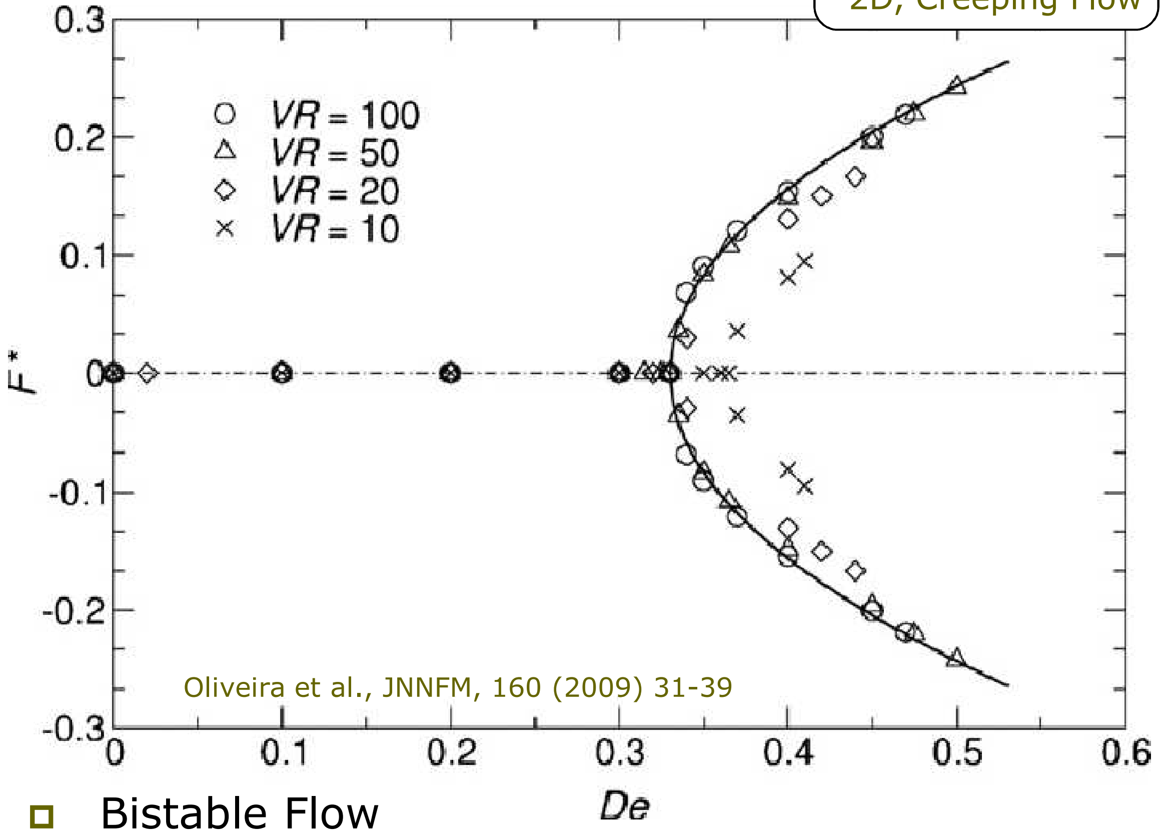

*F**=0 (**symmetric** flow)
F* progressively deviates from *F** = 0 as the flow becomes increasingly asymmetric.

- Bistable Flow
- For high *VR*:
  - De_c **independent of *VR***
  - Evolution of asymmetry independent of *VR*
  - Supercritical pitchfork bifurcation: $F^* = a\sqrt{De - De_c}$

$$= 0.59\sqrt{De - 0.33}$$

Effect of β on the degree of asymmetry

$$\beta \equiv \frac{\eta_s}{\eta_0} = \frac{\eta_s}{\eta_s + \eta_P}$$

$$F^* = \frac{F_W - F_E}{F_3}$$

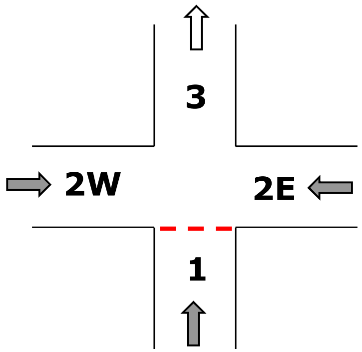

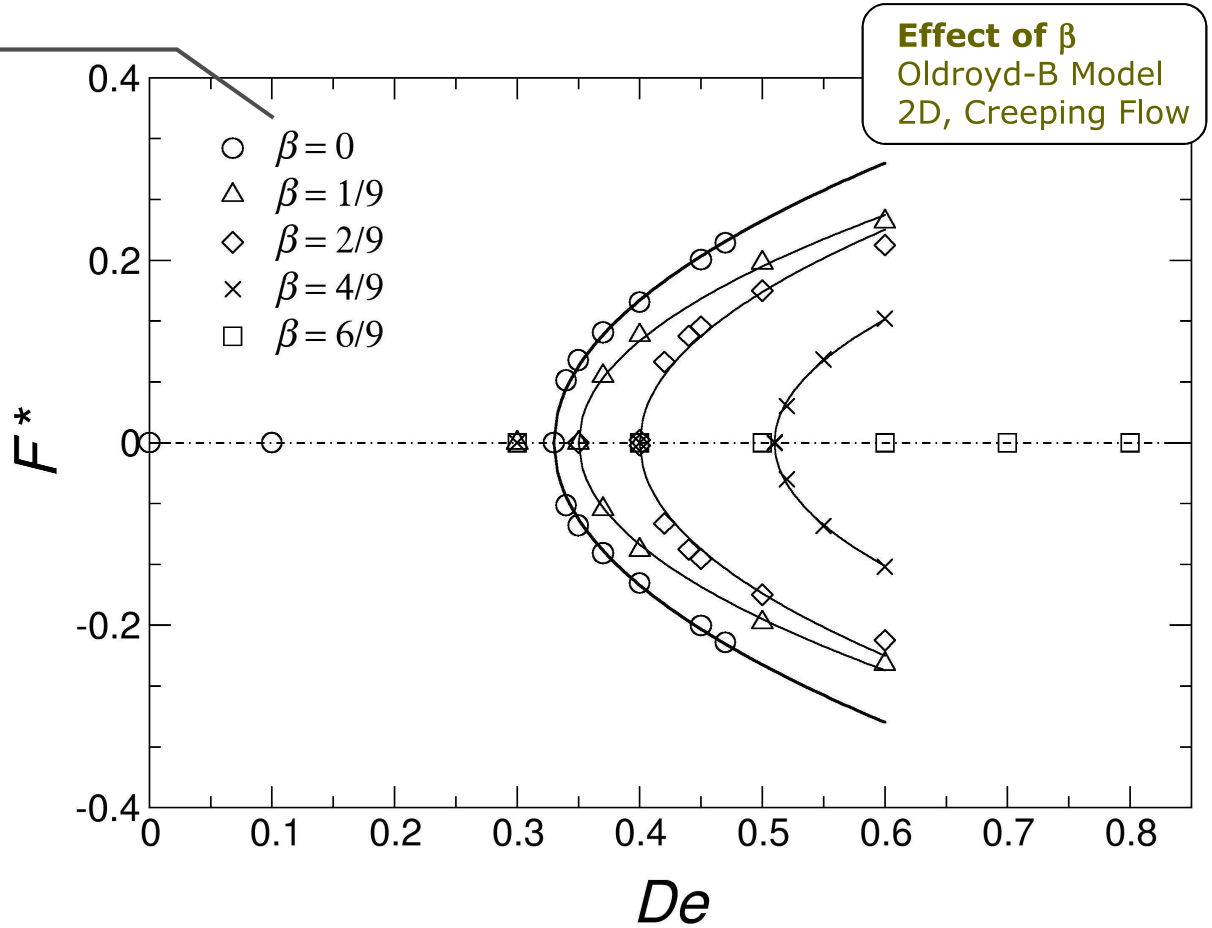

F^*=0 (**symmetric** flow)
F* progressively deviates from $F^* = 0$ as the flow becomes increasingly asymmetric.

- β has a stabilizing effect on the flow:
  - **Increase** in the critical $\boldsymbol{De_c}$
  - For $\beta \geq 6/9$, **no** steady asymmetry is observed.

Effect of ε on the degree of asymmetry

Effect of ε
SPTT Model
2D, Creeping Flow

$$F^* = \frac{F_W - F_E}{F_3}$$

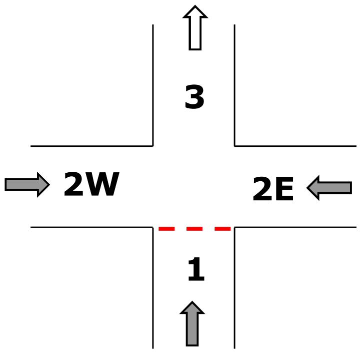

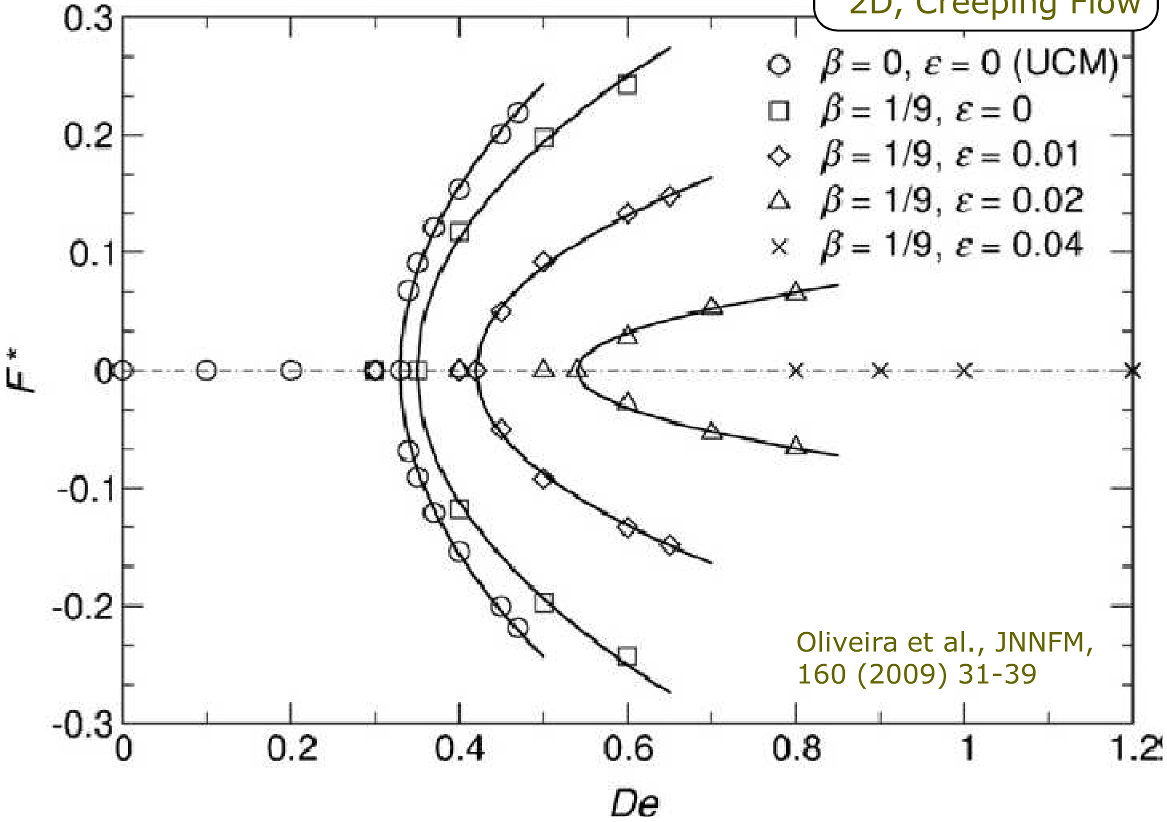

*F**=0 (**symmetric** flow)
F* progressively deviates from *F** = 0 as the flow becomes increasingly asymmetric.

- **Increase** in the critical $\boldsymbol{De_c}$
- Decrease in the degree of asymmetry ($\varepsilon < 0.04$)
- For $\varepsilon \geq 0.04$, the steady asymmetry no longer observed. The flow transitions directly from steady symmetric to unsteady.

Axial Normal Stress Profiles

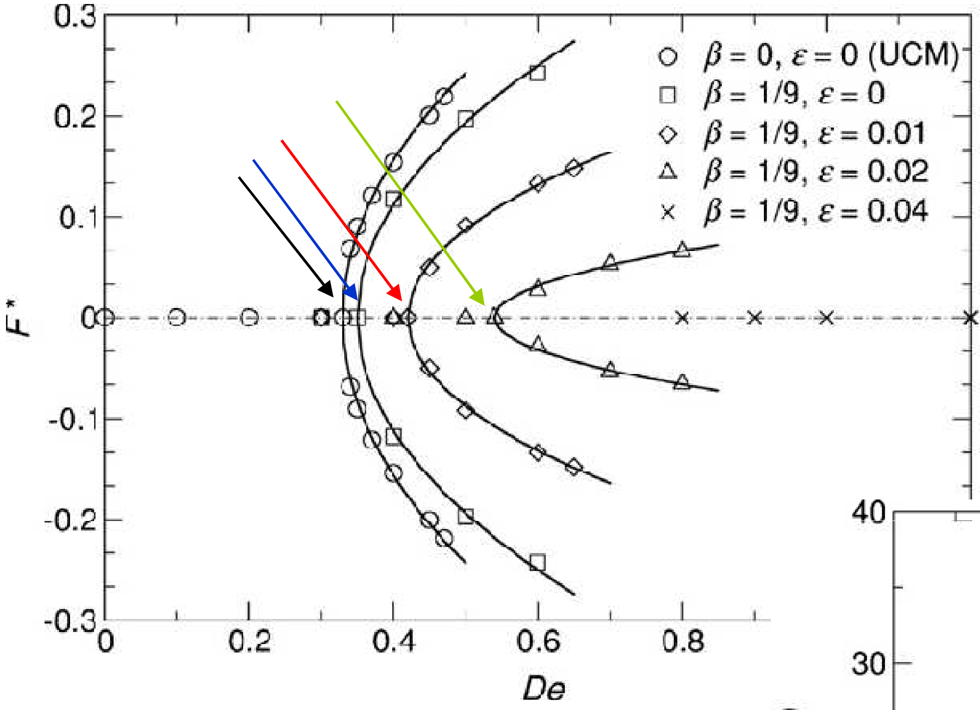

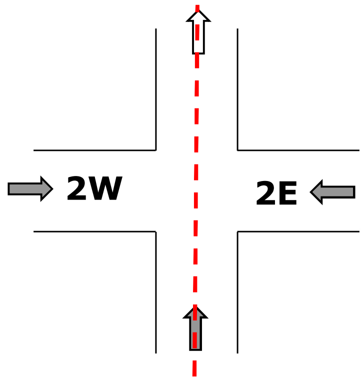

Axial normal stress profiles along the centerline (x = 0)

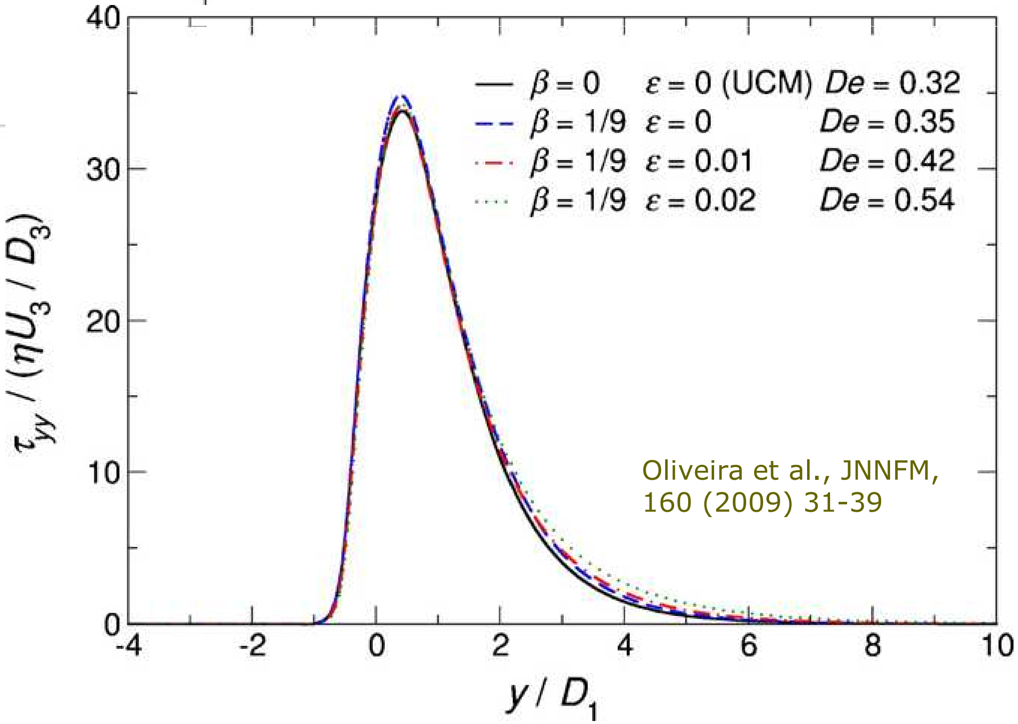

Oliveira et al., JNNFM, 160 (2009) 31-39

- Similar levels of normal stresses achieved near critical conditions.
- Extensional properties decisive for the onset of flow asymmetry.

Viscoelastic Fluid: **PAA125+NaCl**

Q_1 = 0.01 ml/h

increasing Q_2

Viscoelastic

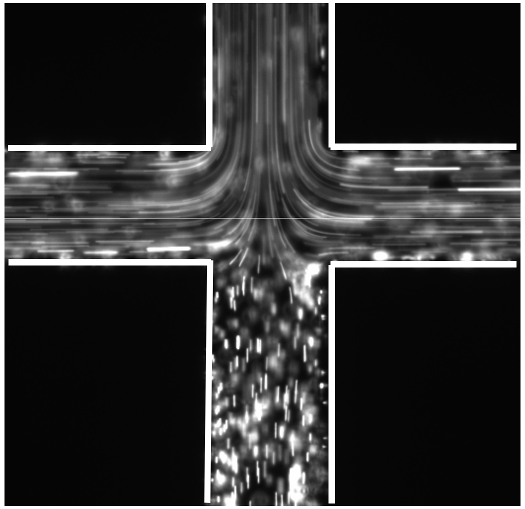

***Q2* = 0.05 ml/h**, *VR* = 5
Re = 0.23, *De* = 0.38

Symmetric

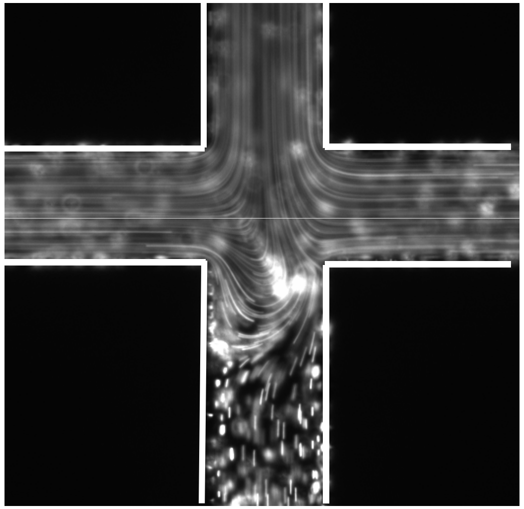

***Q2* = 0.2 ml/h**, VR = 20
Re = 0.87, *De* = 1.41

Steady Asymmetric

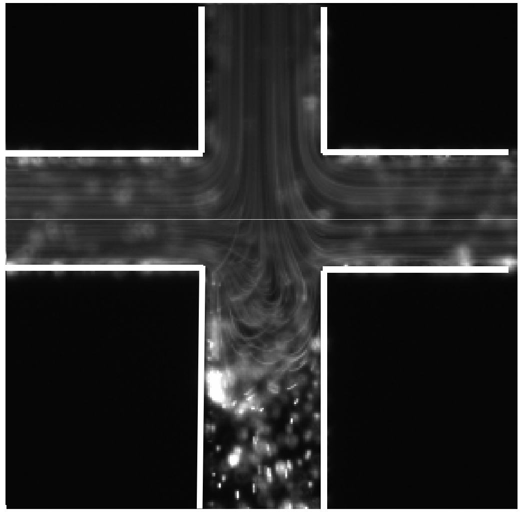

***Q2* = 0.5 ml/h**, VR = 50
Re = 2.15, *De* = 3.479

Unsteady 3D

Viscoelastic Fluid: **PAA125+NaCl**

Q_1 = 0.01 ml/h

Q_2 = 0.05 ml/h, *VR* = 5
Re = 0.23, *De* = 0.38

Q_2 = 0.1 ml/h, VR = 10
Re = 0.45, *De* = 0.723

Q_2 = 0.2 ml/h, VR = 20
Re = 0.87, *De* = 1.41

Viscoelastic

Newtonian

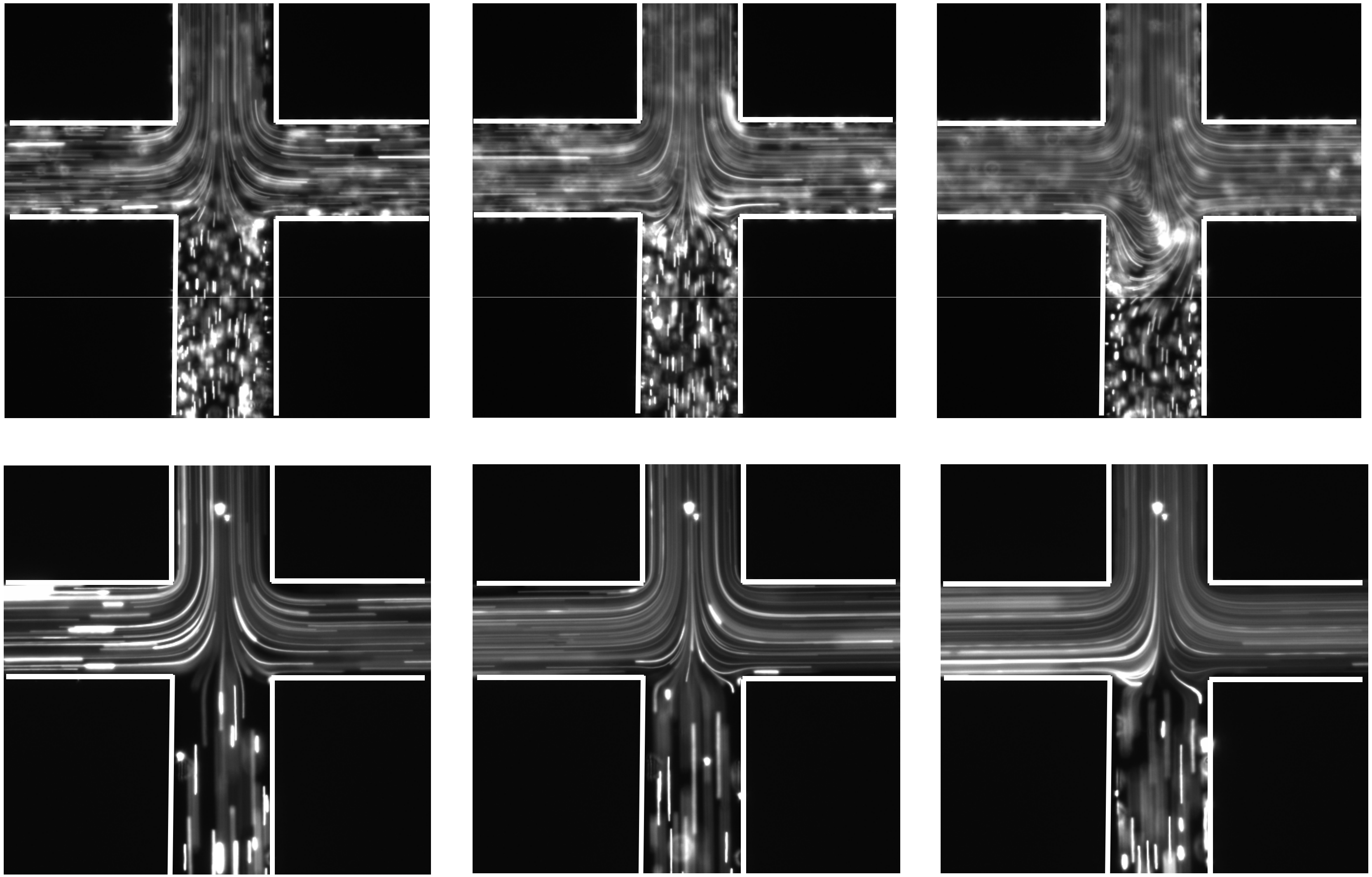

Viscoelastic Fluid: **PAA125+NaCl**

Q_1 = 0.01 ml/h

Viscoelastic Experimental

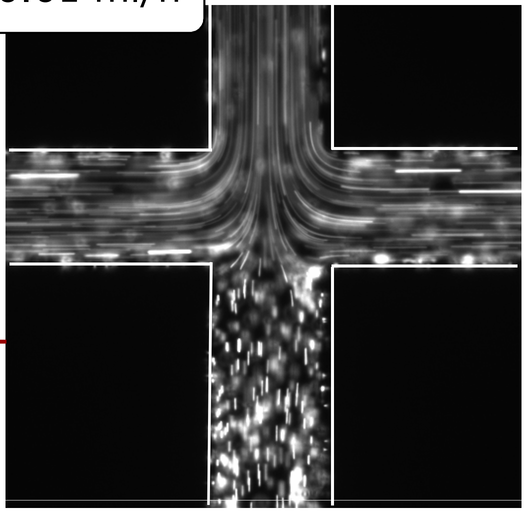

Q2 = 0.05 ml/h, *VR* = 5
Re = 0.23, *De* = 0.38

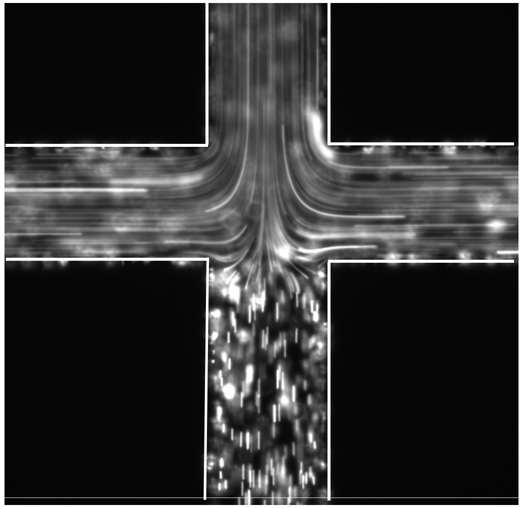

Q2 = 0.1 ml/h, VR = 10
Re = 0.45, *De* = 0.723

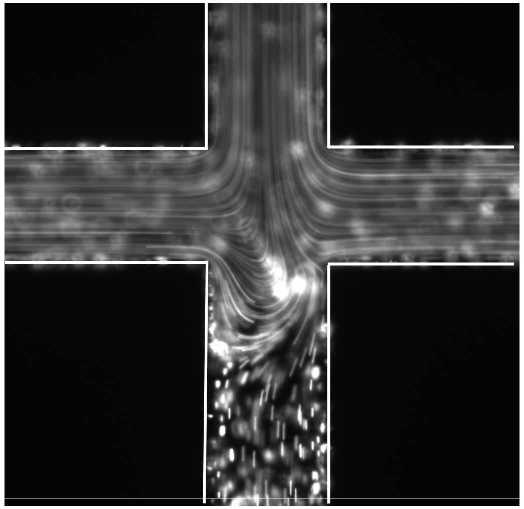

Q2 = 0.2 ml/h, VR = 20
Re = 0.87, *De* = 1.41

UCM 2D Calculations

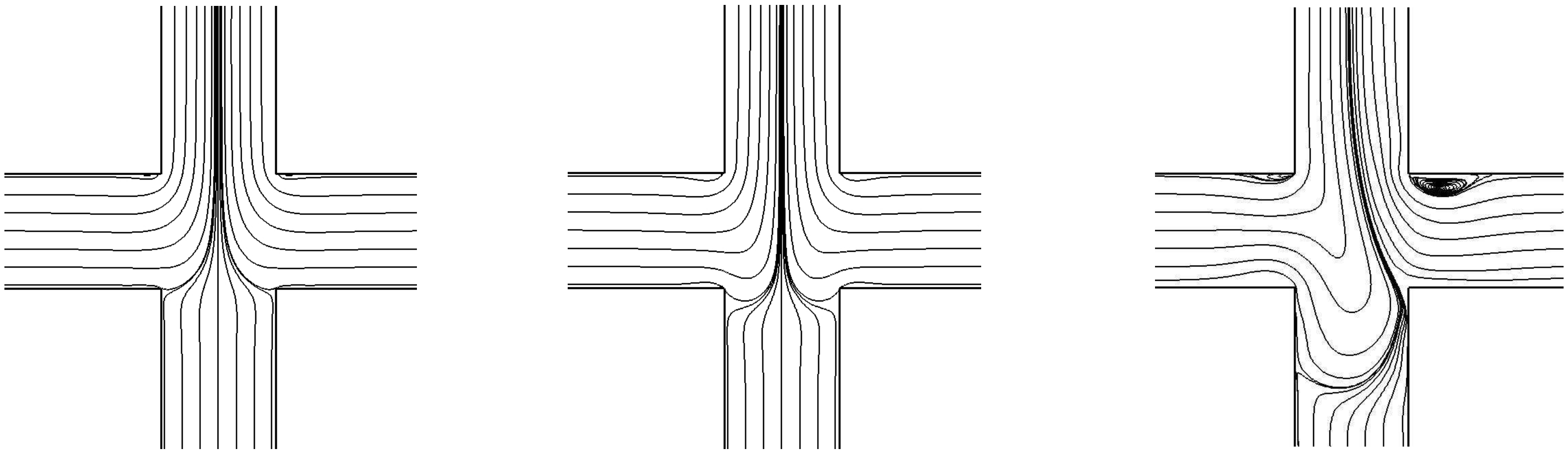

Viscoelastic Model

Q_1 = 0.01 ml/h

UCM
2D Calculations

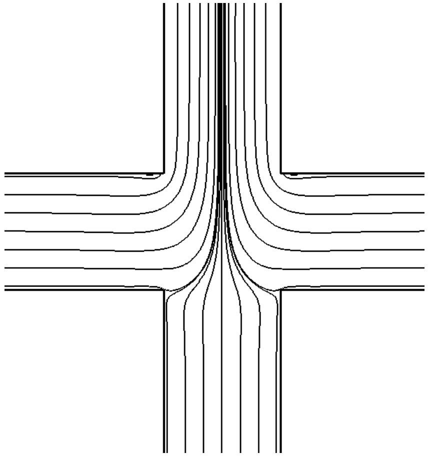

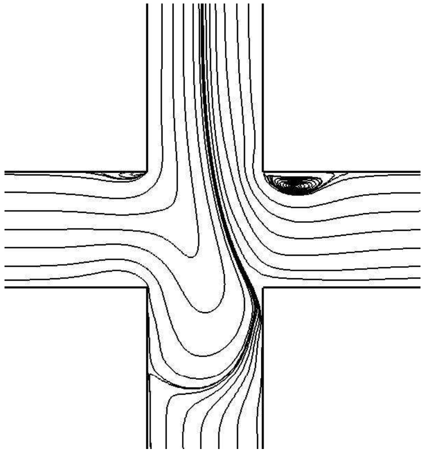

Unsteady 3D

Q_2 = 0.05 ml/h, *VR* = 5
Re = 0.23, *De* = 0.38

Q_2 = 0.2 ml/h, VR = 20
Re = 0.87, *De* = 1.41

Q_2 = 0.35 ml/h, VR = 35
Re = 0.87, *De* = 1.41

Oldroyd-B
2D Calculations

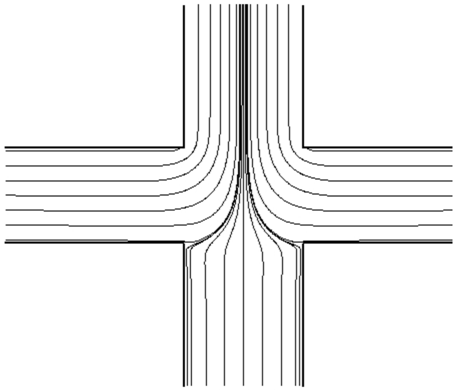

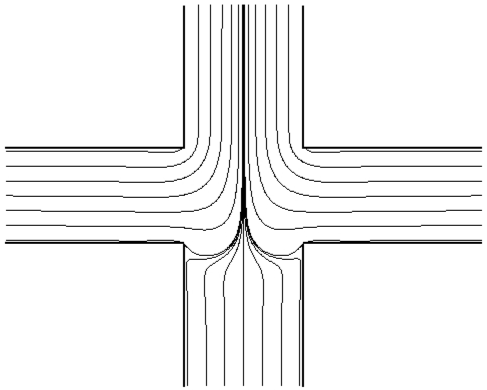

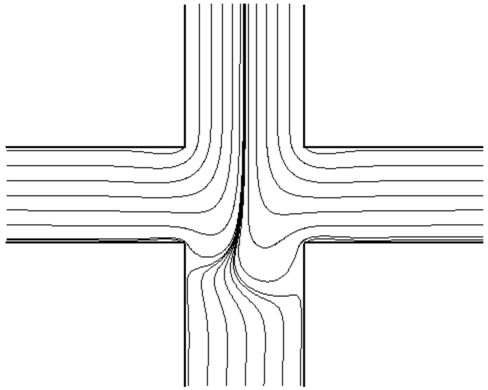

Experimental Flow Map

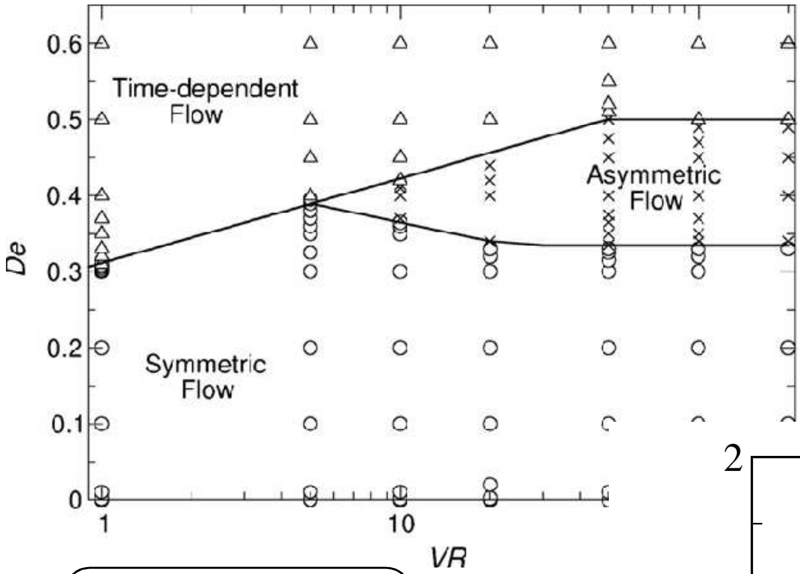

Numeric
UCM Model
2D, Creeping Flow

Experimental
PAA 125 + NaCl

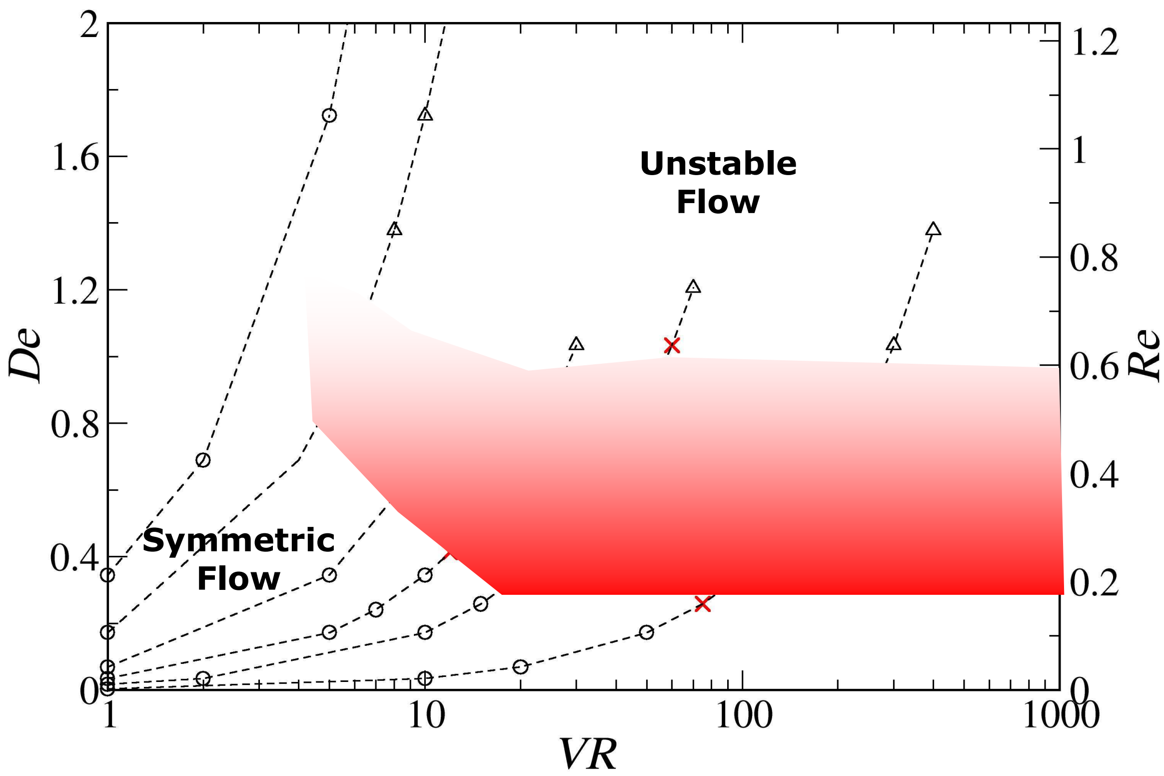

Summary

- Elastically-driven asymmetries at the microscale.
- **Symmetric-breaking bifurcation** at high *De* and *VR.*
- **Unsteady 3D** flow above a critical *De*: useful for mixing purposes.
- Numerical 2D calculations reproduce qualitatively the experimental results.

Ongoing work:

- Experimental: μPIV
- Numerical: 3D simulations

Acknowledgements

- Collaborations:
  - G. H. McKinley, MIT
  - P. J. Oliveira, UBI
  - R. J. Poole, U Liverpool
  - P. C. Sousa, FEUP

- Funding:
  - Fundação para a Ciência e a Tecnologia and FEDER (Portugal) under projects:
    - PTDC/EQU-FTT/71800/2006
    - PTDC/EQU-FTT/70727/2006